JOURNAL OF MATERIALS SCIENCE 15 (1980) 188–196

Adherence properties of metal-to-ceramic joints

R. F. PABST, G. ELSSNER
Max-Planck-Institut für Metallforschung, Institut für Werkstoffwissenschaften, Stuttgart, Germany

A study is reported of the fracture mechanics of metal-to-ceramic laminates (Al_2O_3/Nb, Si_3N_4/Zr) produced by solid-state bonding. The bond quality of notched bend and tension specimens is described in terms of a stress intensity factor K_{ICV}, which is evaluated in the same way as for isotropic material. K_{ICV} is measured as functions of the microstructure of the constituents, the metal layer thickness, the environmental conditions and the test temperature. At very high test temperatures where plastic flow occurs, the J-integral was used for bond quality characterization. For the linear elastic case, the J-value is compared with the stress intensity concept K_{ICV}. In contrast to the behaviour of a bulk ceramic material, the J-value increases with increasing test temperature if a thick metal layer (3 mm) is used.

1. Introduction

High-temperature technology has placed increasing demands on structural members of ceramic materials and metal-to-ceramic joints. For application, metal-to-ceramic joints must have suitable strength properties at 1300 K and higher. At room temperature, metal-to-ceramic joints are especially needed in the field of biomaterials.

The soundness of the ceramic-to-metal joints must be assured to guarantee the performance of the structure in which they are incorporated. Tests to determine the bond strength properties are, therefore, of major importance for the assessment of the quality of the bond and the development of metal-to-ceramic composites.

The mechanical testing of metal-to-ceramic joints is normally conducted by conventional tensile and bend tests or by peel tests [1]. These methods provide bond strength data which are functions of the specimen size and the test method employed. What is needed, however, are bond strength data which may be regarded as materials constants only influenced by fabrication parameters and parameters such as chemical and mechanical compatibility, intrinsic material properties and local characteristics such as macroscopic flaws. This may be provided by fracture mechanics test methods yielding values which accurately describe the fracture resistance of the bond. These methods have been applied to the solid-state bonded metal-to-ceramic joints under present consideration.

2. Problems of brittle bond strength measurements

An understanding of the critical nature of the bond is necessary for a general understanding of the composite performance. Laminated composites are comprised of a ceramic substrate and a single relatively thin metal foil; the combination may be designated as brittle. The bond quality of the components is governed by stress concentrations at microscopic defects of flaws at the interface which lead to rupture with very little subcritical crack extension or plastic deformation.

Assuming a dispersion of defects flaws at the interface, conventional bend and tensile tests on smoothed (unnotched) specimens provide data which are a function of the size of the bonded interface under load [2]. Such a dependence may be accounted for by statistical variations. Statistical methods are, however, very elaborate and require many observations relating to the structure of the bonding interface. Also, bonded joints are susceptible to failures at the free surfaces; cracking may occur at these singular points. In addition, if the bond strength is much higher than the strength of the ceramic constituent, the unnotched specimen

 0022–2461/80/010188–09$02.90/0

TABLE I Materials used for solid-state bonded metal-to-ceramic joints. Test temperature: room temperature

Material	Composition (wt%)	Density ($g\,cm^{-3}$)	Grain size $\bar{d}$ (μm)	K_{IC} ($MN\,m^{-3/2}$)	K_{ICV} ($MN\,m^{-3/2}$)
alumina					[a]
I	99.7	3.82	5	4.4[b]	0
II	99.7	3.83	4	4.4[b]	0
III	99.7	3.78	6	3.6	5.6 3.7
IV	97 + 3 SiO_2	3.70	10	3.5	5.9[c] 4.5[d]
V	99.7	3.80	15	3.4	3.2
VI	99.7	3.84	20	2.7	2.3–3.5
VII	99.7	3.32	2	0.8	3.2
VIII	99.7	3.58	2	0.8	1.7–2.5
IX	99.7	3.95	11	3.3	1.8
HP silicon nitride	2.5 MgO; 5 SiO_2	3.18	1–7	5.5	1.9[e]

Niobium 99.82 Nb, vacuum depressed at 2450 K; 78 VHN (load 0.5 N). $K_{IC}(Nb) = 12\,MN\,m^{-3/2}$ (embrittled).
Zirconium 99.97 Zr, cold-worked; 190 VHN (load 0.5 N).
[a] Except as noted, all values are for 0.1 mm Nb foil with notch along the interface.
[b] Inhomogeneous grain-size distribution. Some grains as large as 50 μm.
[c] 1 mm Nb foil, notch in the midplane of the Nb foil.
[d] 3 mm Nb foil.
[e] 0.5 mm Zr foil.

will fail away from the joint region. In all cases the normal conventional and statistical assumptions are not suitable [3].

A much more promising approach consists in the description of an artificially introduced crack or notch developing at the bonded interface. The fracture resistance of the crack should then characterize the bond strength independent of the interface size. An analysis of adherence should be feasible, therefore, with fracture mechanics techniques. These techniques give a more scientific footing for bond strength measurements and have already found application in adherence studies of polymer adhesives [4] and glass-bonded thick-film conductors [5].

The formalism of linear fracture mechanics is valid primarily for isotropic materials. It is also possible to describe the fracture behaviour of an anisotropic structure. Nevertheless, the anisotropic analysis of a laminated structure is, in particular, highly complex. It is noted that the stress intensity generally depends upon the elastic properties of the constituents, the crack length and the layer thickness. If a perfect bond exists (no flaws and defects at the interface) the open mode fracture toughness of the bond K_{ICV} (V = Verbindung = joint) may be computed by theory from the bulk fracture toughness values K_{IC} of the constituents and a function $\ominus (E_i, \nu_i)$ which describes the influence of the elastic properties [6].

Experimentally, K_{ICV} may be measured for an arbitrary bond strength in the same way as for an isotropic material with an artificial crack or notch at or near the interface. Then, K_{ICV} characterizes the bond quality with the understanding that:

(1) the crack runs paralled to the bonded interface;

(2) the stresses and strains are proportional to the inverse square root of the distance r from the crack tip;

(3) there exists a correction function Y such that K_{ICV} is independent of specimen geometry and crack length;

(4) the influence of asymmetry, as the crack elongates at the interface and not at the midplane of the layer is neglected [6].

3. Experimental procedure

3.1. Materials

The composite test pieces were fabricated of polycrystalline alumina parts (Table I) with high-purity niobium foil as an intermediate layer. Niobium has favourable chemical and mechanical compatibility with Al_2O_3 and a relatively high melting point [7].

A second layered composite system consisting

of hot-pressed Si_3N_4 and a zirconium foil as a layer was studied. This system is distinguished from the Al_2O_3/Nb system in that the laminate forms intermediate reaction products of silicide during the welding process [8].

3.2. Fabrication process

Laminated composites of two rectangular bodies and a metal foil were welded together in high vacuum by induction heating. The solid-state bonding process is implemented by application of thermal and strain energy. It is essential that the experimental rig is designed so that any possibility of poor alignment is excluded during the welding process [9]. This becomes increasingly difficult with increasing specimen length and an enhanced rate of shrinkage (with porous ceramic materials) as well as an increasing flow at elevated temperatures. On the other hand, especially in the case of a foil of a refractory metal, flow of the ceramic component is necessary to obtain closely fitting surfaces.

Measurements have shown that for reproducible bond quality, a uniform pressure distribution and a constant temperature profile in the plane of the joint surface are necessary conditions [10]. However, a specific temperature gradient perpendicular to the welded surface is also necessary; this temperature gradient confines the zone of plasticity to a narrow region near the interface and prevents instability of the test set-up during the welding process [9].

3.3. Specimen preparation

The dimensions of the welded area were 18 mm × 11 mm. The length of the welded specimen was 60 mm. One welded specimen was used to obtain four or five bend specimens of dimensions 7.0 mm × 3.5 mm × 60 mm. Notches of width $w = 50\,\mu m$ and depth a were introduced at the metal-to-ceramic interface by a precision diamond cutting device [9] (Fig. 1).

Four-point loading instead of three-point loading was used to minimize shear and wedging effects at the interface region [11] (Fig. 2).

For comparison, round tensile specimens 60 mm long, 5 mm thick were obtained from an identical welded specimen. Round notches of width $w = 50\,\mu m$ were introduced at the metal-to-ceramic interface for K_{ICV} determination (Fig. 2a).

4. Results and discussion

4.1. Effect of test method

Table II shows fracture toughness data K_{IC} of a bulk ceramic material evaluated from tension and bend specimens and K_{ICV} data of an Al_2O_3/Nb composite. For both specimen configurations, similar values can be expected for K_{ICV} if the bond quality is the same.

The lower K_{IC} values for the tensile test of the bulk material are due to superimposed bending moments caused by eccentric loading of the test specimen. The larger differences in bend and tensile K_{ICV} data can be attributed to additional superimposed moments caused by eccentric (asym-

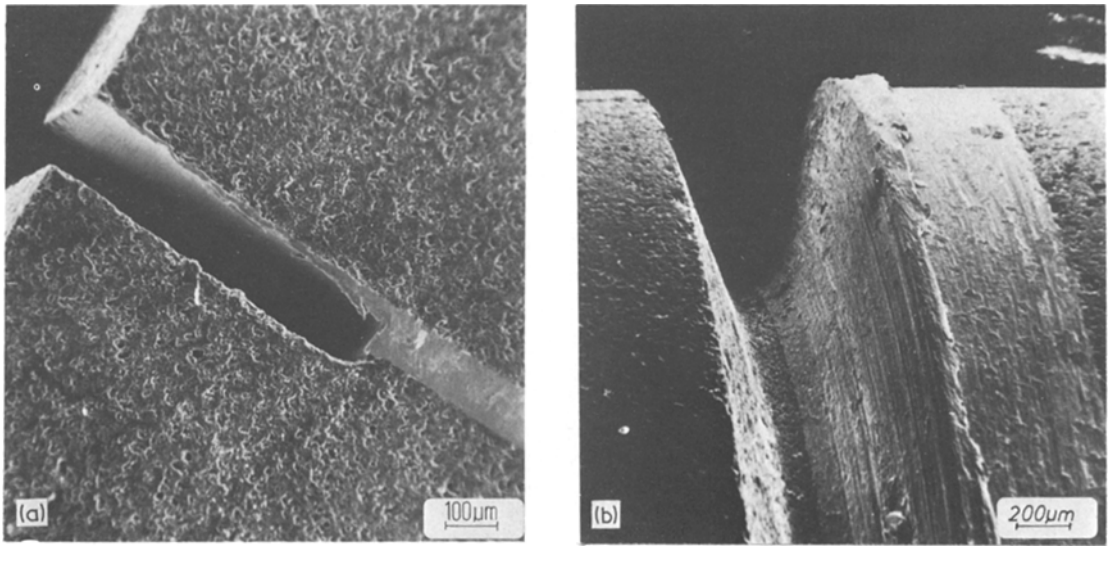

Figure 1 Notches at the ceramic-to-metal interface for (a) bend test, and (b) tensile specimens.

TABLE II Comparison of fracture resistance data K_{ICV} for an Al_2O_3 IX/Nb joint and for the corresponding fracture toughness K_{IC} of an Al_2O_3 IX bulk material

Material	Bend test	Tensile test
Al_2O_3 IX (Table I)	$K_{IC} = 3.25$ (± 4%) $MN^{3/2}$ (11 specimens)	$K_{IC} = 2.89$ (± 9%) (11 specimens)
Al_2O_3 IX/Nb	$K_{ICV} = 1.84$ (± 19%) (26 specimens)	$K_{ICV} = 1.43$ (± 26%) (27 specimens)

Welding time, 2 h; welding pressure, 64 MPa; welding temperature, 2000 K; Nb foil thickness, 1 mm.

metrical) unbonded areas in the welded surface [12].

With increasing welding pressure at elevated temperatures, the risk of surface sliding and shearing increases. The bond strength is then lowered and the K_{ICV} data may deviate systematically with position along the welded surfaces as shown in Fig. 3.

4.2. External and internal parameters

External parameters such as welding time, temperature and pressure are of limited moderate importance as long as intimate contact of the surfaces is reached [13]. The same can be stated about the influence of the finishing of the mating surfaces [7]; gross mismatch which prevents intimate contact cannot be permitted.

K_{ICV} depends heavily on internal parameters such as grain size (grain-size distribution) porosity and impurity content. Large grains meeting at the interface act as flaws with stress concentrations due to the inability of these large grains to flow and make intimate contact with the mating surface. These microstructural features which influence the brittle interface defect structure are as important as the chemical and mechanical compatibility of the constituents [14, 15].

The influence of the microstructure of the ceramic constituent on the K_{ICV} data are summarized in Table I. For comparison, K_{ICV} data of a Si_3N_4/Zr welded joint are included. For highly porous alumina materials, such as alumina VIII, the K_{ICV} values of the bond may exceed the fracture toughness K_{IC} of the ceramic-base material by a factor of 2 or 3. This is because of an excellent matching of the surfaces and a highly effective bonding due to the plastic flow of the porous ceramic constituent at bonding temperatures. For the dense alumina which exhibits a high K_{IC} value of the base material (alumina I, II) very weak joints are formed. However, for the dense alumina which exhibits a somewhat lower K_{IC} value, joints with excellent properties (K_{ICV}) are fabricated. Since all of these dense materials were of similar mean grain size and chemical purity, the differences in K_{ICV} values could not be attributed to differences in plastic flow. However, microstructural examination revealed that the alumina which formed low-strength joints consisted of fine-grained material ($\approx 1\,\mu m$) which had a few very large grains ($\approx 50\,\mu m$) whereas the high K_{ICV} joints were formed by alumina with a homogeneous fine-grained microstructure. It is felt that the inability of single large grains to

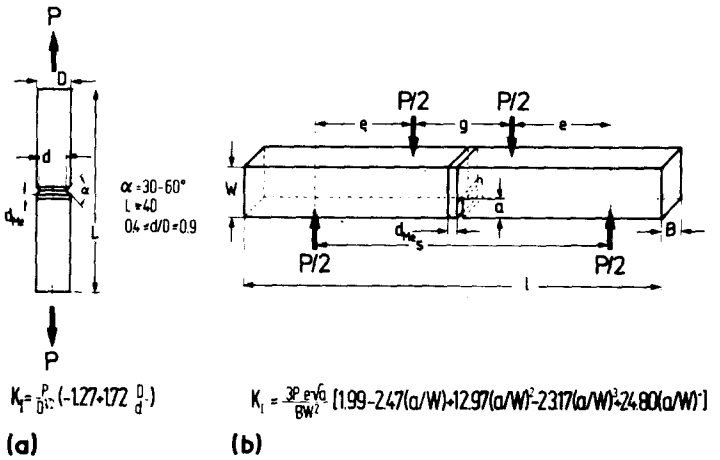

Figure 2 Test configurations for K_{ICV} measurements. (a) Four-point bend test, (b) tensile test. d_{Me} = metal layer.

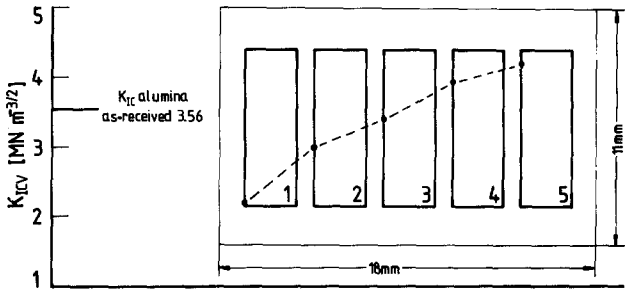

Figure 3 K_{ICV} as a function of location of the test specimens (1 to 5) within the welded area (18 mm × 11 mm). One welded specimen was used to obtain four or five bend-test specimens.

deform at welding temperatures causes unbonded areas at the interface which act as flaws.

4.3. Cohesive and adhesive fracture and layer thickness effects

There exist four types of fracture paths which depend on the microstructure of the interface [16]:

(1) composites with fine-grained high-density alumina, fracture exactly along the interface;

(2) joints consisting of a metal layer and a highly porous ceramic or joints which had suffered a thermal fatigue, fracture within the ceramic part but very near to the interface;

(3) in structures where the metal foil was seriously embrittled by oxygen diffusion (alumina IV), the crack runs within the metal foil;

(4) the Si_3N_4/Zr laminate shows an intermediate layer system consisting of a silicide, and a Zr transformation structure. In this particular case the crack alternates from one side of the silicide to the other (Fig. 4).

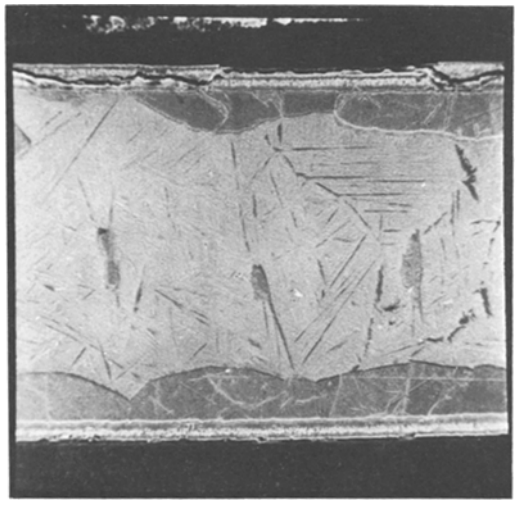

Figure 4 Alternating crack path for a Si_3N_4–Zr laminated joint.

Traditionally, fracture which occurs exactly at the interface is defined as adhesive and that which occurs at some distance from the interface is defined as cohesive. However, since (if a finite bond exists) the elastic properties of the bonded materials and the layer thickness have an effect on the fracture toughness in the joint region, adhesive fracture could perhaps be better defined as fracture which occurs at or near the interface which does not have the same fracture toughness as the bulk material. The measured K_{ICV} data for different fracture paths gives some indication of this behaviour: for a fracture path near to the interface but completely within the ceramic constituent the measured fracture toughness is higher than that of the bulk ceramic. Similarly for a fracture path completely within the tin Nb foil (0.1 mm thick) the measured fracture toughness is only as high as the bulk value of the ceramic constituent and much lower than the bulk niobium (Table I). Even for a 1 mm layer, the bulk fracture toughness value of Nb is not reached. This behaviour is due to the difference in elastic properties of the two materials, the bond quality and the layer thickness.

Fig. 5 shows the K_{ICV} dependence of crack location for an alumina with a 3% glassy phase. The niobium layer thickness was 1 mm. For comparison a theoretical curve for perfect bond is drawn [17]. As mentioned above, even in a 1 mm thick niobium layer the K_{IC} value of the bulk material is not reached. The measured value is lower than the theoretical prediction. The minimum value of K_{ICV} is not reached at the interface of the joint but at some distance within the ceramic part. Such behaviour needs further consideration. It is assumed that the ceramic near to the interface is weakened during the welding

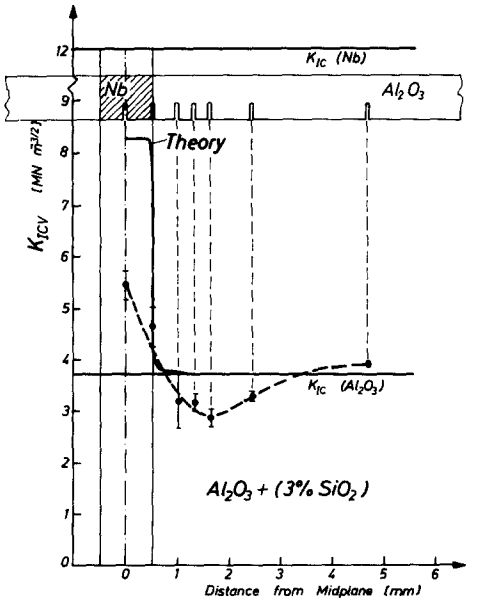

Figure 5 K_{IC} as a function of notch location. The theoretical curve is computed for a perfect bond [17]. The bulk value K_{IC} (Nb) is not reached for a crack running within the Nb layer.

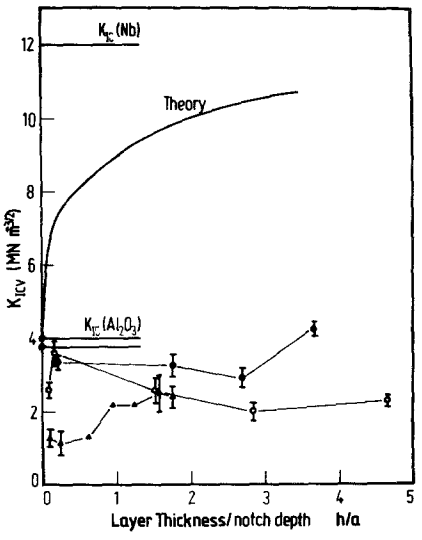

Figure 6 Comparison of computed and measured values of K_{ICV} as functions of ratio h/a (h = layer thickness, a = notch length) and the alumina quality. Welding conditions: welding temperature, welding time, welding pressure: ▲ Al_2O_3 99.7%/Nb, 1970 K – 2 h – 31 MPa; • Al_2O_3 99.7%/Nb, 2000 K – 1 h – 12 MPa; ○ Al_2O_3 97.0% + 3% SiO_2/Nb, 1970 K – 2 h – 32 MPa.

processes. Investigation of the structure of the ceramic at some distance from the interface shows a more inhomogeneous grain distribution and some texture. At a distance of about 4 mm from the midplane of the joint, the K_{IC} value of the bulk ceramic material is reached.

4.4. Layer thickness and defect structure

As a consequence of the elastic mismatch, the K_{ICV} value should increase with increasing metal layer thickness for a fixed notch location as shown by the theoretical curve in Fig. 6. This curve was computed from the K_{IC} values of the constituents assuming that the bond is perfect, i.e. no weak-bonded areas exist at the interface [18].

The measured K_{ICV} values plotted in Fig. 6 as a function of layer thickness and for a notch at the interface are ambiguous showing an overall increase as expected (alumina ▲) but also a certain minimum (alumina •) or even an overall decrease of K_{ICV} (alumina ○). The unexpected behaviour is a function of the changing brittle defect structure with increasing metal layer thickness. Scanning electron microscopy reveals that the niobium grains grow during the welding process to a size that is limited only by the layer thickness (Fig. 7); as the layer thickness increases the grain size also increases. Since these large niobium grains can act as flaws, increasing the grain size can increase the flaw size thus decreasing the bond strength. As previously discussed, a competing mechanism is that of increasing bond strength with increasing layer thickness due to elastic interactions between the materials. The combination of these two phenomena plus those of the defect structure of the ceramic, ultimately determines the bond strength. Debased alumina (alumina ○) enhances the effect of defect length due to reaction with the niobium foil resulting in oxygen embrittlement of the foil; a pronounced decrease of K_{ICV} with increasing layer thickness was found.

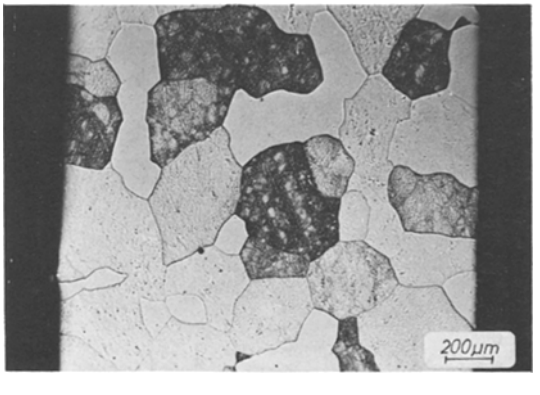

Figure 7 SEM of large grains within the niobium layer.

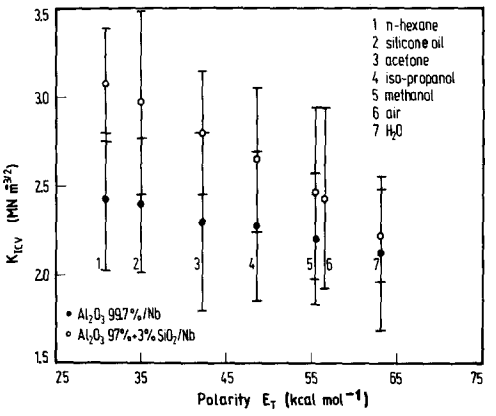

Figure 8 K_{ICV} as a function of various environments characterized by its polarity E_T. Parameter, pure 99.7% and debased 97% alumina.

4.5. Influence of environment

K_{ICV} data were measured as functions of different environment characterized by its polarity E_T [19] (Fig. 8). The test specimens were impregnated at a rough vacuum state in a special impregnation chamber which minimized the water content at the notch tip.

K_{ICV} decreases with increasing polarity as a function of the alumina quality used [20]. The decrease is a function of the silica content and is more pronounced for alumina with a high SiO_2 content than for more pure alumina. Since the environmental influence on K_{ICV} values affects the life-time of the composite, an effort should be made to measure physical parameters in conditions which closely approximate the expected service conditions.

TABLE III K_{ICV} as a function of test temperature T_t. Al_2O_3/Nb-joint. Nb-foil-thickness is 1.0 mm. Testing in a high vacuum (1×10^{-4} Pa)

Joint parameters	Test temperature T_t (K)	K_{ICV} (MN m$^{-3/2}$)
Al_2O_3 IX/Nb	295	2.0
Welding temperature	1070	2.4
$T_W = 2000$ K	1270	1.5
Welding pressure	1470	1.5
$P = 5 \times 10^6$ Pa	1770	0.8

4.6. Influence of temperature

Metal-to-ceramic joints are mostly needed in the field of high-temperature technology. Therefore, K_{ICV} data as a function of the test temperature were determined for Al_2O_3/Nb and Si_3N_4/Zr adhesive joints, using notched specimens and three-point loading.

Table III reveals that the Al_2O_3 IX–Nb composite has considerable bond strength up to 1970 K in vacuum. The crack in the notched specimen runs precisely at the interface at ambient and elevated temperatures. Comparable measurements with bulk alumina [21] showed a steeper decrease in K_{IC} values with temperature. It must be concluded that the metal layer has a certain supporting function to the joint.

At higher temperatures, load–deflection curves become non-linear (Fig. 9). To evaluate real K_{ICV} data at these higher temperatures, the non-linearity must be considered [22]. For this case the J-integral was used to characterize the bond strength at high temperatures. In the linear elastic region up to $T_1 = 1173$ K, the critical J-value, J_{ICV}, may be

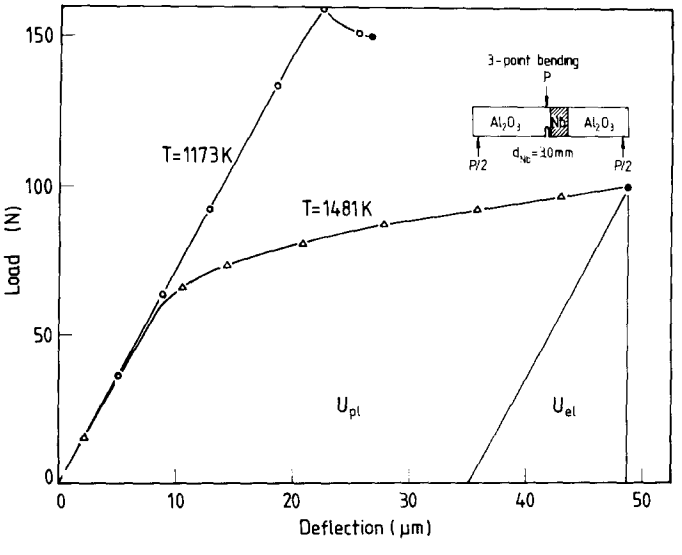

Figure 9 Linear elastic and plastic behaviour of Al_2O_3/Nb joints tested at $T_1 = 1173$ K and $T_2 = 1481$ K. Metal-layer thickness $d_{Nb} = 3$ mm. The diagram was used for J-integral computations.

TABLE IV Comparison of bond strength data K^*_{ICV} (*J*-integral) and K_{ICV} (SIK) for linear elastic behaviour ($T_1 = 1173$ K). For non-linear behaviour ($T_2 = 1481$ K) only the *J*-integral can be used

Test temperature	*J*-integral [22]				SIK
	(1) K^*_{ICV}	(2) K^*_{ICV}	(3) K^*_{ICV}	(4) K^*_{ICV}	K_{ICV}
$T_1 = 1173$ K	1.30	2.56	2.51	2.57	2.58
$T_2 = 1481$ K	4.45	4.74		4.64	
	Nb – foil = 3 mm				

(1) $J = 2(U_1 - U_3)Q_R$
(2) $J = 2U_1/Q_R; U_3 = 0$
(3) $J = C_1 \cdot U_1 + C_2 U_2 - C_3 U_3)/Q_R$
(4) $J = G + 2 \cdot U_{pl}/Q_R \dfrac{(w - a_1)}{(w - a_0)}$.

Where U_i = stored strain energies, C_i = constant, $Q_R = B(W - a_0)$, B = specimen thickness, W = width of the specimen, a_0 = initial crack length, a_1 = critical length, $U_1 = U_{plastic} + U_{elastic}$, $U_2 = P \cdot \delta - U_1$, P = load, δ = deflection, $U_3 = U$ (without an artificial notch), G = crack extension force for linear elastic behaviour, K^*_{ICV} = evaluated from *J*-integral, and K_{ICV} = stress-intensity concept (SIK).

compared with K_{ICV} of a stress intensity concept. This is done in Table IV for different methods. There is an excellent agreement of K^*_{ICV} values estimated from the *J*-integral and the directly measured K_{ICV} (SIK) value for methods 2 and 4. At $T_2 = 1481$ K, the stress–strain behaviour was non-linear. Only the *J*-integral concept could be used to evaluate K_{ICV}. The K_{ICV} data at this temperature, T_2, proved to be much higher than in the linear elastic case. This is in contradiction to the behaviour of bulk ceramic material and metal-to-ceramic joints with thin ($\approx$ 1 mm) metal layers. It confirms the conclusion that the metal layers may have a supporting function to the joint, which increases with increasing layer thickness at high temperatures. Also, with decreasing layer thickness, the high-temperature behaviour approaches the characteristic of a bulk ceramic material.

5. Concluding remarks

Although the analysis of a laminated structure is highly complex, if the influence of asymmetry is neglected, the anisotropic K_{ICV} factor may be measured in the same way as for isotropic materials. This calculated K_{ICV} factor gives a more scientific footing for bond strength measurements and accurately describes the bond quality of metal-to-ceramic joints. However, in the high-temperature region where plastic flow occurs, the characterization of bond quality with *J*-integral appears to be suitable.

These techniques have helped to describe the influence of microstructure in the interfacial region, environmental effects and layer thickness effects. Nevertheless, there remains much to be done, especially in the theoretical field, to account for the effects of anisotropy and imperfect bonding at the interface.

References

1. H. E. PATTEE, WCR Bulletin No. 148, Welding Research Council, New York (1972).
2. R. F. PABST, *Z. Werkstoff.* **6** (1) (1975) 17.
3. W. WEIBULL, *Ing. Vetenskaps Akad. Handl.* (1939) 153.
4. E. J. RIPLING, S. MOSTOVOY and R. L. PATRICK, *Mat. Res. Stand.* **4** (3) (1964) 129.
5. P. F. BECHER and W. L. NEWELL, *J. Mater. Sci.* **12** (1977) 90.
6. R. F. PABST and G. ELSSNER, to be published.
7. G. ELSSNER, R. PABST and J. PUHR-WESTERHEIDE, *Z. Werkstoff.* **2** (1974) 61.
8. G. ELSSNER, R. F. PABST and S. ALDINGER, *Prakt. Metallogr. Sonderband* **6** (1976) 274.
9. R. F. PABST and K.-D. MÖRGENTHALER, *Z. Werkstoff.* **2** (1976) 62.
10. G. ELSSNER and R. F. PABST, *High Temp. High Press.* **6** (3) (1974) 321.
11. R. F. PABST, *Berichte DKG* **54** (12) (1977) 391.
12. K.-D. MÖRGENTHALER, Dissertation, University of Stuttgart (1979).
13. G. ELSSNER, K.-D. MÖRGENTHALER and R. F. PABST, *Fachberichte Tagung Verbundwerkstoffe, Konstanz* (1974) 415.
14. G. ELSSNER and R. F. PABST, *Proc. Brit. Ceram. Soc.* **25** (1975) 179.
15. R. F. PABST and G. ELSSNER, *Sci. Ceram.* **7** (1975) 73.
16. G. ELSSNER, S. RIEDEL and R. F. PABST, *Prakt. Metallogr.* **12** (1975) 234.
17. R. F. PABST and G. ELSSNER, to be published.

18. F. ERDOGAN, G. D. GUPTA and T. S. COOK, "Numerical solution of singular integral equations, Mechanics of fracture 1", edited by G. C. Sih (Noordhoff, Leyden, 1973).
19. R. F. PABST, G. WICHMANN and G. ELSSNER, *Adv. Biomater., Eval. Biomater.* **1** (1979) to be published.
20. F. BARISCH, Master-Thesis, University of Stuttgart (1975).
21. N. CLAUSSEN, R. F. PABST and C. -P. LAHMANN, *Proc. Brit. Ceram. Soc.* **25** (1975) 139.
22. R. F. PABST, G. ELSSNER and U. KROHN, *Berichte der DKG* **55** (12) (1978) 518.
Received 18 May and accepted 6 June 1979.